

# The Generation and Confinement of Relativistic Electrons at the WEGA Stellarator

H. P. Laqua<sup>1</sup>, E. Chlechowicz<sup>2</sup>, M. Dostal<sup>3</sup>, M. Otte<sup>1</sup> and T. Stange<sup>1</sup>,

<sup>1</sup>Max Planck Institute for Plasma Physics, EURATOM Association, 17491 Greifswald, Germany

<sup>2</sup>HSX Plasma Laboratory, University of Wisconsin, Madison, USA

<sup>3</sup>University Rostock, 18055 Rostock, Germany

**Introduction:** A toroidal magnetic configuration with helically twisted magnetic field lines confines ionized energetic particles with a parallel momentum  $mv_{\parallel}$ . In a stellarator this configuration is established solely through the use of external coils. As long as the centrifugal force  $F_{cf}$  is negligible with respect to the radial magnetic field force  $F_m$  ( $mv_{\parallel}^2/R \ll qv_{\parallel}B_{\theta}$ ), the particle orbits remain on the magnetic flux surfaces. Here  $R$  represents the radial position,  $q$  the charge and  $B_{\theta}$  the poloidal component of the magnetic field, which generates the rotational transform of the field lines. For higher parallel momentum the particle orbits deviate from the flux surfaces, but form their own closed drift surfaces [1]. In the case that  $F_{cf}$  points in the same direction as  $F_m$ , the drift surfaces are larger than the flux surfaces and the orbits can exceed the confinement region and the particles may be lost by collision with the vacuum vessel. When  $F_m$  acts against  $F_{cf}$ , the drift surfaces are displaced towards the torus outboard side and shrink in radius with increasing parallel momentum as shown in **Fig. 1**. The anisotropic confinement of the “runaway” orbits generates a net toroidal current [2].

**Experimental set-up:** WEGA is a classical five period and  $l = 2$  stellarator with a major radius of 0.72 m and an aspect ratio of 7. It is equipped with toroidal field coils and two oppositely energized helical field coils that generate the rotational transform  $\iota$  and thus the closed magnetic flux surfaces. The discharge length at 0.5 T is up to 20 s, which allows operating the plasma in a stationary state. WEGA is equipped with a 10 kW (cw) electron cyclotron resonance heating (ECRH) system at a frequency of 28 GHz and a 9 MHz (3 kW) ion cyclotron wave heating ICH by means of a single loop antenna. ECRH and ICH are supported by a 20 kW (cw) non-resonant 2.45GHz microwave system with a TE11 waveguide antenna with a diameter of 89 mm and a double cut at its front as described in [3]. This antenna generates an electric field of up to 100 kV/m with a polarization parallel to the magnetic field lines and a narrow  $N_{\parallel}$  spectrum ( $N_{\parallel} < 1$ ). The generated supra-thermal electron component was identified by its microwave, soft X-ray (sX) and  $\gamma$ -ray emission. The  $\gamma$ -ray emission is measured with a Geiger-Müller-type detector (Gamma-Scout™) using the lead filter method. The detector is screened by a 100 mm thick lead tube with different lead foils at its front, pointing towards the source of highest emission. The microwave emission is detected by a 12 channel absolutely calibrated radiometer with a spectral range between 22 and 40 GHz. The plasma current is measured by a Rogowski coil.

**Experimental results:** The plasma is initiated by 28 GHz ECRH at a magnetic flux density  $B_0$  of 0.5 T on axis with Helium or Hydrogen as the working gas. The plasma density is of the order of  $1-2 \times 10^{18} \text{ m}^{-3}$ . Once the plasma is established, the 2.45 GHz non-resonant heating is applied additionally. With increasing power a toroidal current of several hundred Amps is established, accompanied by broadband microwave radiation similar to synchrotron radiation with an observed radiation temperature of up to 1keV, continuous soft-X-ray emission with energies up to the detection limit of 200 keV and the emission of  $\gamma$ -radiation. The spectral decay of the synchrotron radiation indicates the existence of 2 MeV electrons. Once the 2.45 GHz heating power has reached the flat top, the 28 GHz ECRH is switched-off and the stationary plasma is sustained solely by the 2.45 GHz microwave power for several seconds as shown in **Fig. 2**. The plasma could be alternatively initiated by ICH breakdown. In other discharges the toroidal field  $B_0$  is varied (0.2- 0.5T), while keeping the poloidal field constant and vice versa. In both cases the rotational transform is varied. Even though fast particle trajectories strongly deviate from the field lines, their confinement shows a similar  $\iota$  dependence as a high temperature plasma in a low shear stellarator. The fast particles close to the antenna field are detected by a movable probe. The position of residence zone and the particle confinement are compared with the appearance of large islands at low rational surfaces in the confinement region. When large islands appear in front of the antenna the coupling is perturbed and the plasma current and synchrotron emission show a minimum.

**Modeling:** The acceleration mechanism of the electrons is assumed to be based on a stochastic process taking place when the relativistic electrons pass the antenna RF-field similar to that described in [4]. The size of the antenna pattern close to its mouth is about half the vacuum wavelength. This means that electrons with a parallel velocity close to  $c$  can interact with the RF-field most efficiently. Whether there is an energy gain or loss depends on the phase relation between the electron position and the RF-field. Outside of this zone the electrons lose any phase information, since the time to encircle the torus ( $\tau_{\text{tor. orbit}}$ ) is more than 40 times longer than the RF cycle, the orbits are not closed (no rational rotation transform) and the electrons collide with the bulk electrons, ions and neutrals. The effect of many passages can be described as a diffusion process in energy space thus changing the distribution function of the electrons (EDF) in a statistical way. The corresponding random walk in energy space corresponds to a diffusion coefficient,  $D(E) = \langle |\Delta E| \rangle_E^2 / (2\tau_{\text{tor. orbit}})$  shown in **Fig. 3**, where  $\langle |\Delta E| \rangle_E$  is the average absolute energy step of an electron with kinetic energy  $E$ .  $D(E)$  is calculated by solving the relativistic momentum equation of the electrons in the RF-field. The average is taken over the phase of the RF-field when the particles enter the field region. The electric field amplitude is calculated from the launched RF-power (3 kW), taking into account the reflection at the cut-off density.

With this diffusion coefficient, the diffusion equation for the electron energy distribution function

$$\frac{\partial f}{\partial t} = \frac{\partial}{\partial E} \left( D(t, E) \frac{\partial f}{\partial E} \right) - (c_{\text{Rutherford}} E^{-3/2} - c_{\text{inelastic}}) f$$

is solved including the loss terms due to coulomb ( $\sim E^{1.5}$ ) and inelastic collisions with neutrals as shown in **Fig. 3**. The simulation is initialized with a Maxwellian EDF at the onset of the 2.45 GHz heating. Fortunately, the characteristic time constants for the EDF relaxation is much longer ( $>20$  ms, see exponential decay in **Fig. 2**) than the diffusion time constant ( $<1$  ms) and therefore these processes are separated in short pulse modulation experiments. Further, we calculate the average energy increase per time and particle. Multiplying this by the total number of the particles involved ( $3 \times 10^{13} - 2.1 \times 10^{14}$ ), a lower and upper limit of the absorbed power is obtained, being of the order of 0.15-1 kW, which is a noticeable fraction of the input power of 3 kW. The interaction with the RF-field leads to a tail formation in the EDF, which remarkably takes quite a long time (in the order of milliseconds as shown in **Fig. 3**). This result is corroborated in modulated power experiments (see **Fig. 4**). The RF-power of 3 kW is switched on for 1.5 ms and switched down to about 150 W for 15 ms repeatedly. A time delay for the high energy tail ( $\gamma > 5$ ) formation is deduced from the synchrotron radiation, which is emitted by those electrons only. For the plasma current which is driven by all accelerated electrons, the model predicts an immediate linear increase when the power is switched on. This is also observed in the experiment. The current starts to decay immediately when the power is switched down, which can be associated with a current that is driven by all non-thermal electrons. In this case the large number of “low” energy electrons dominates the signal. If a loss term is introduced into the diffusion equation, the model reproduces the decay of the plasma current after switching down the power.

For the explanation of the strong  $\iota$  dependence the island structure in front of the antenna was introduced in the coupling model. The larger the island size the larger becomes the plasma antenna distance. The position of the fast particles is also found more inward shifted. The electric field decays exponentially with the antenna plasma distance. Therefore the strong variation with  $\iota$  can be explained by the variation of the antenna coupling. The confinement of the fast electrons was not affected by the rotational transform since the decay time of the plasma current and synchrotron radiation did not show any  $\iota$  dependence after the 2.45 GHz switch-off.

**Summary and conclusion:** The generation of relativistic electrons can be explained by the stochastic interaction of relativistic electrons with the 2.45 GHz RF-field at the antenna mouth. The toroidal plasma current is a result of the different confinement properties of co- and counter moving electrons. The  $\iota$  dependence exists due to the changing island formation in front of the antenna.

### References:

- [1] Zehrfeld H. P., Fussmann B. and Green B. J.; Plasma Physics. Vol. 23, No. 5, pp. 473 to 489, 1981.
- [2] Laqua. H.P. et al. Plasma Phys. Control. Fusion, 56,(2014) 075022 (6pp)
- [3] Podoba Y.Y, et al. : PRL **98**, 255003 (2007).
- [4] Fuchs V. et al. Submitted to Phys. Plasmas

## Figures:

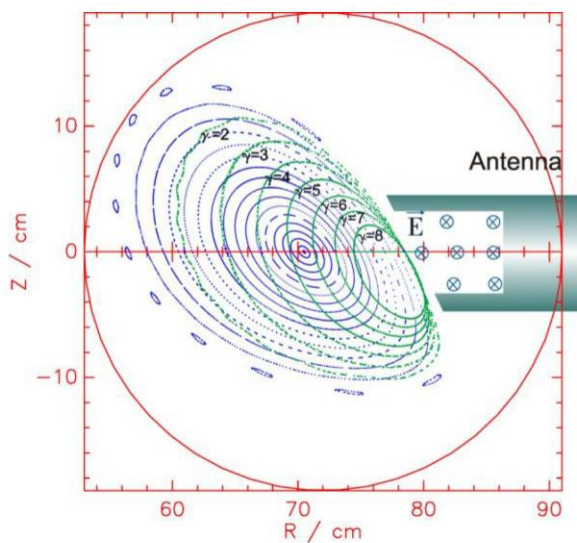


**Figure 1:** Flux surfaces (blue) and particle drift surfaces (green) for different relativistic  $\gamma$ -factors. On the right there is a simplified sketch of the antenna field.

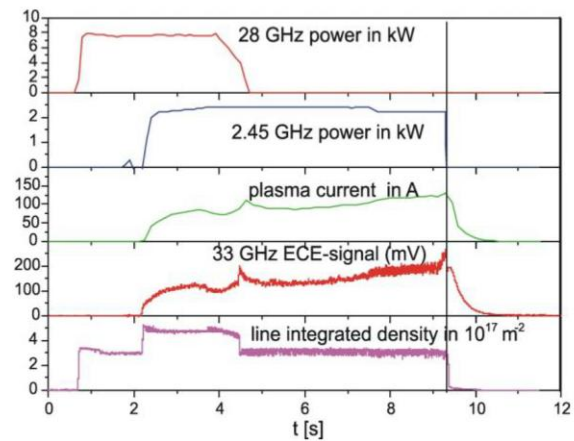


**Figure 2:** Heating scenario: Start-up with 28GHz ECRH at 0.5T up to  $t = 4.5$  s. Pure non-resonant 2.45 GHz heating and current drive is established up to 9.3 s. Thereafter an exponential decay is seen in the plasma current and synchrotron radiation.

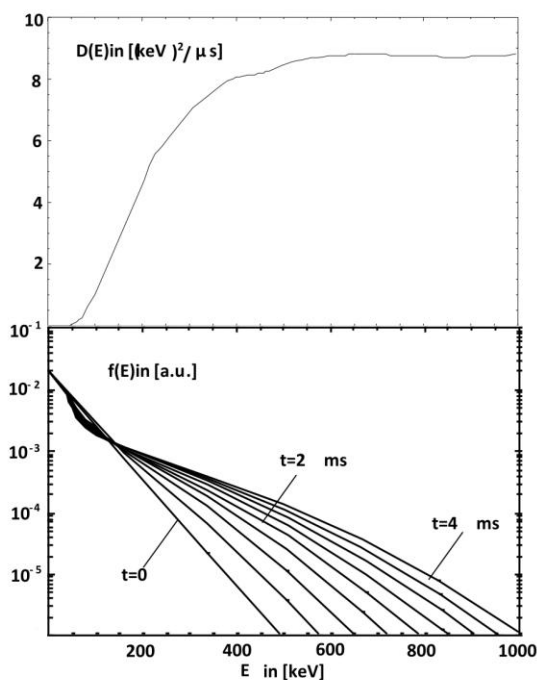


**Figure 3** top: Diffusion coefficient  $D(E)$  vs. kin. Energy. bottom: Tail formation by diffusion of a Maxwellian EDF ( $T_e = 50$  keV) using  $D(E)$ .

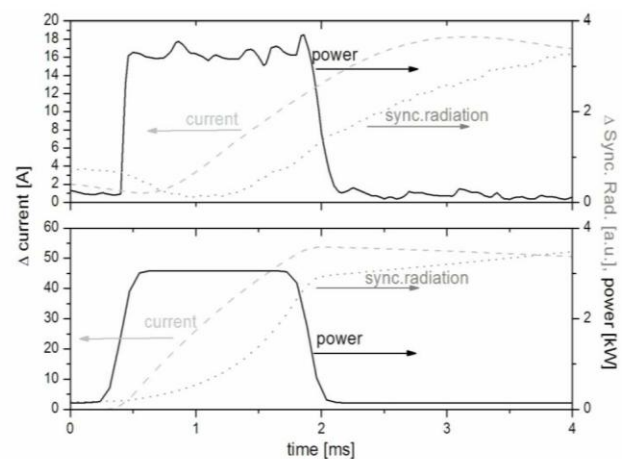


**Figure 4:** Comparison of experiment (top) and modelling (bottom). Time evolution of the plasma current (dashed) and synchrotron radiation (dots) when the heating power (solid) is modulated.